A SEMI-ANALYTICAL MODEL FOR THE PREDICTION OF THE BEHAVIOR OF TURBULENT COAXIAL GASEOUS JETS

by

Amin LOTFIANI *, Shahram KHALILARYA, and Samad JAFARMADAR

Mechanical Engineering Department, Urmia University, Urmia, Iran

Original scientific paper
DOI: 10.2298/TSCI110701140L

In diffusion combustion systems, fuel and oxidizer (usually air) are admitted into the combustion chamber separately in the form of turbulent jets. Most often, fuel enters the furnace from a round nozzle and air is admitted through an annulus surrounding the central fuel nozzle. Momentum of the fuel and air jets is utilized for directing the flame and controlling the mixture formation which is typically the rate-limiting step of the combustion process. Hence the behavior of turbulent coaxial jets must be well understood prior to any detailed analysis of these systems. In this study, a set of relations is proposed to predict the behavior of turbulent coaxial gaseous jets using curve-fits to the computational fluid dynamics solutions and the fluid flow governing equations as well as the ideal gas equation of state. A computer program is developed to implement the presented model. Results are compared with existing data and reasonable agreement is observed. According to the results, the presented model makes sufficiently accurate estimates of the flow and concentration fields in a very short time.

Key words: *coaxial jets, semi-analytical model, turbulent mixing, diffusion combustion*

Introduction

In diffusion combustion systems, the length and shape of the flame depend to a large extent on the mixing process between the fuel and air, which enter the furnace separately, in the form of turbulent jets. The rate of mixing depends on the flow characteristics. Therefore, modeling studies of time mean average properties of the flow such as velocity and species concentration enable us to predict the flame characteristics and the effect of different flow parameters on the combustion process. Usually, fuel enters the combustion chamber from a round nozzle and air is admitted through an annulus surrounding the central fuel nozzle. Momentum of the fuel and air jets is utilized for directing the flame and controlling the mixture formation which is typically the rate-limiting step of the combustion process. Thus, it is necessary to study the behavior of turbulent coaxial jets prior to any detailed analysis of diffusion combustion systems. Because of the symmetry of such coaxial jets about their axis, they can be treated as 2-D for the purpose of analysis.

Previous research on turbulent coaxial jets includes, among others, the experimental study of Forstall and Shapiro [1] who seeded helium into the inner jet and used a gas sample probe to measure gas concentration and a Pitot probe to measure velocity. Morton [2] performed a theoretical analysis and proposed a differential equation method to predict the concentration and velocity profiles. Due to a number of major assumptions, experimental agreement with his

* Corresponding author; e-mail: a.lotfiani@urmia.ac.ir

model was poor. Chigier and Beer [3] experimentally studied the near-field of air-air coaxial jets. Williams *et al*. [4] studied air-air coaxial jets in order to decrease the noise from jet engines. Pressure measurements were made using an impact tube with a disk-type static probe from which velocity profiles were obtained. Concentration measurements were made by seeding CO_2 into the outer jet. Champagne and Wygnanski [5] expanded the work of Chigier and Beer by measuring the mean velocities, turbulence intensities, and shear stresses for coaxial jets using two linearized constant temperature anemometers. Ribeiro and Whitelaw [6] investigated coaxial jets with and without swirl using a hot-wire anemometer. Ko and Kwan [7] made an effort to understand the underlying vortical structures in the near-field of coaxial jets. They utilized a pressure probe, a hot-wire anemometer and microphone spectra in their study. Dahm *et al*. [8] directly imaged the vortex structures and dynamics using two-color planar laser induced fluorescence (PLIF). Buresti *et al.* [9] studied air-air coaxial jets and used laser Doppler anemometry (LDA) and hot-wire measurements to obtain velocity statistics. Warda *et al.* [10] studied the influence of various parameters such as the initial velocities on the flow field of air-air coaxial jets using LDA. Because of their relation to rocket injectors, non-reacting and reacting coaxial jets with properties typical of such injectors have been investigated by Schumaker [11] using PLIF. Enjalbert *et al*. [12] presented an entrainment model for turbulent jets in a co-flow in the self-similar region, based on the Taylor entrainment hypothesis. They assumed that the axial velocity component follows a Gaussian distribution. Antoine *et al.* [13] investigated the mass transport properties of a round jet of water discharging into a low velocity co-flowing water stream, experimentally. Measurements were performed in the self-similar region of the jet.

The aim of this research is to propose a set of simple relations for the prediction of the behavior of turbulent coaxial gaseous jets. Computational fluid dynamics (CFD) simulations are carried out to yield further insights into the problem. It has been previously demonstrated that, when properly implemented for the case of interest, CFD solution is reliable [14, 15]. The continuity and momentum equations as well as the ideal gas equation of state are employed to derive the desired expressions. Curve-fits to the CFD solutions are used to determine the experimental constants. A computer program is developed in Matlab 7.1 to implement the presented model. Results are compared with existing data and reasonable agreement is observed.

Velocity on the centerline of the jet

Fuel and air are injected through a round nozzle and an annulus surrounding the central fuel nozzle, respectively, into the still ambient air. The jet fluids and the ambient air are at the same temperature. Physical observations and dimensional analysis lead us to the following hyperbola for the estimation of the velocity on the centerline of the jet:

$$\frac{v_c}{v_f} = \frac{1}{a_0 + a_1 \dfrac{x}{d_1}} \tag{1}$$

where v_c is the velocity on the centerline of the jet, v_f – the velocity at the fuel nozzle exit, x – the axial distance from the fuel nozzle exit, d_1 – the fuel nozzle diameter, and a_0 and a_1 are dimensionless constants. The smaller diameter of the annular air nozzle equals d_1 and the larger diameter is d_2.

In this model, values greater than 1 obtained for v_c/v_f from eq. (1) are replaced with 1. This substitution implies that we are in the potential core of the jet. As soon as the value of v_c/v_f becomes smaller than 1, no substitution is made and we have passed through the potential core.

Hence the length of the potential core is unknown *a priori* and may vary, depending on the case considered. The quantities in this paper are time-averaged ones.

From dimensional analysis, a_0 and a_1 are found to be functions of the density ratio and the momentum ratio. The density ratio is the ratio of the ambient fluid (air) density to the round jet fluid (fuel) density, $DR = \rho_a/\rho_f$. The momentum ratio is the ratio of the annular jet momentum to the round jet momentum, $MR = \dot{m}_{a,inj} v_a/\dot{m}_f v_f$. Here, $\dot{m}_{a,inj}$ is the mass flow rate of air injected through the annular nozzle and $\dot{m}_f$ is the mass flow rate of fuel injected through the round nozzle. v_a is the velocity at the annular (air) nozzle exit. It is assumed that a_0 and a_1 can be expressed as products of two distinct functions each of which depends on only the density ratio or the momentum ratio. Thus:

$$a_0 = f_0(DR)g_0(MR) \tag{2}$$

$$a_1 = f_1(DR)g_1(MR) \tag{3}$$

In the continue, we try to find relations for f_0, g_0, f_1, and g_1. To that end, first the momentum ratio is set to zero (single round jet) and the corresponding values of g_0 and g_1 are assumed to be equal to 1. The optimum values of and at different density ratios are determined using the least squares method. The shape of f_0 and f_1 can be deduced from the variations in a_0 and a_1. The next stage is to find the optimum values of a_0 and a_1 at different momentum ratios, while keeping the density ratio constant. Comparing these values a_0 and a_1 with those corresponding to the zero momentum ratio, g_0 and g_1 are determined.

To perform the above-mentioned procedure, several cases with different density and momentum ratios are simulated using a CFD flow solver. Details of the CFD solution are given in the subsequent sections. Problem specifications in the cases with zero momentum ratio are shown in tab. 1. Table 2 shows the required data for the cases with different momentum ratios. Reynolds number, Re_1 given in these tables is based on the inner jet parameters.

Table 1. Problem specifications in the cases with zero momentum ratio

Round jet fluid	*DR*	d_1 [mm]	d_2 [mm]	ρ_a [kgm^{-3}]	ρ_f [kgm^{-3}]	v_a [ms^{-1}]	v_f [ms^{-1}]	Re_1
Hydrogen	14.371	10	50	1.177	0.0819	0	20	1844
Methane	1.805	10	50	1.177	0.652	0	20	11679
Acetylene	1.112	10	50	1.177	1.058	0	20	20946
Air	1.000	10	50	1.177	1.177	0	20	13076
Ethane	0.963	10	50	1.177	1.222	0	20	26127
Propane	0.657	10	50	1.177	1.791	0	20	43812
Butane	0.498	10	50	1.177	2.362	0	20	63039

According to the results, the following relations are proposed for f_0, f_1, g_0, and g_1, as indicated in fig. 1:

$$f_0 = -0.1274\left(\frac{\rho_a}{\rho_f}\right) + 0.6934 \tag{4}$$

$$f_1 = 0.1695\left(\frac{\rho_a}{\rho_f}\right)^{0.436} \tag{5}$$

$$g_0 = \left(\frac{\dot{m}_{a,inj} v_a}{\dot{m}_f v_f} + 1\right)^{-1.907} \tag{6}$$

Table 2. Required data for the cases with different momentum ratios

DR	*MR*	d_1 [mm]	d_2 [mm]	v_a [ms^{-1}]	v_f [ms^{-1}]	Re_1
1.805	0.25	10	50	1.52	20	11679
1.805	0.50	10	50	2.15	20	11679
1.805	0.75	10	50	2.63	20	11679
1.805	1.00	10	50	3.04	20	11679
1.805	1.25	10	50	3.40	20	11679
1.805	1.50	10	50	3.72	20	11679
1.805	1.75	10	50	4.02	20	11679
1.805	2.00	10	50	4.30	20	11679
1.805	2.25	10	50	4.56	20	11679
1.805	2.50	10	50	4.80	20	11679

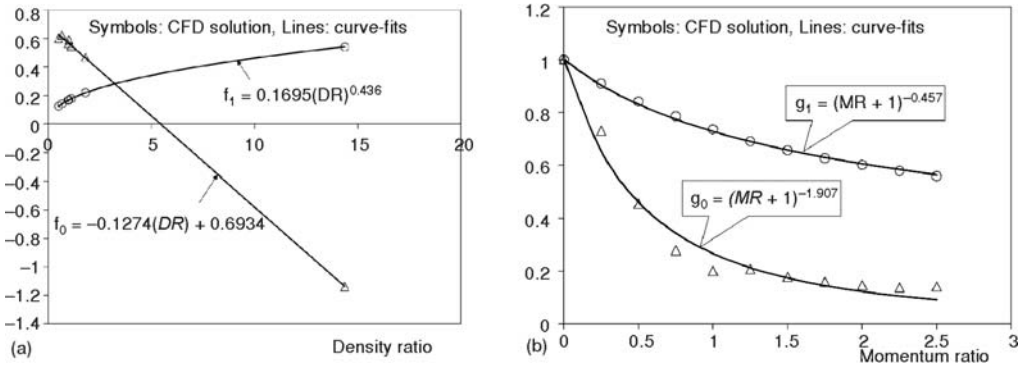

Figure 1. Determination of f_0, f_1, g_0, and g_1 using curve-fits to the CFD solution

$$g_1 = \left(\frac{\dot{m}_{a,inj} v_a}{\dot{m}_f v_f} + 1 \right)^{-0.457} \tag{7}$$

Therefore, a_0 and a_1 in eq. (1) can be calculated as:

$$a_0 = \left[-0.1274 \left(\frac{\rho_a}{\rho_f} \right) + 0.6934 \right] \left(\frac{\dot{m}_{a,inj} v_a}{\dot{m}_f v_f} \right)^{-1.907} \tag{8}$$

$$a_1 = 0.1695 \left(\frac{\rho_a}{\rho_f} \right)^{0.436} \left(\frac{\dot{m}_{a,inj} v_a}{\dot{m}_f v_f} \right)^{-0.457} \tag{9}$$

Velocity on the centerline of the coaxial jets can be easily estimated using eqs. (1), (8), and (9). Results show that the average discrepancy between the velocity values predicted by the present model and those obtained from the CFD solution does not exceed 0.005 v_f.

Boundary of the jet and entrainment of air

Having predicted the velocity on the symmetry axis, boundary of the jet can be determined using the mass and momentum conservation equations together with the ideal gas equa-

tion of state. The axial velocity component and the fuel concentration are very small at the boundary of the jet. Figure 2 shows the boundary of the jet and the co-ordinate system used, as well as the control volume applied in the analysis.

Radial distribution of the axial velocity at any cross-section of the jet is assumed to follow a Gaussian profile as:

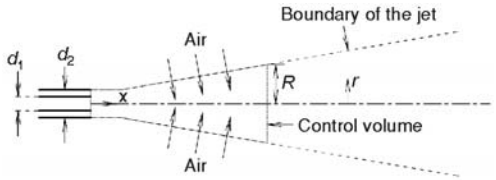

Figure 2. Schematic view of the boundary of the jet, the co-ordinate system, and the control volume used

$$\frac{v}{v_c} = \exp\left[-k_v\left(\frac{r}{R}\right)^2\right] \tag{10}$$

The same assumption has been frequently made by researchers in the fully-developed region of jets (*e. g.* see [12, 13, 16]). In eq. (10), v is the axial velocity at the point (x, r), v_c – the velocity on the symmetry axis at the point (x, 0), r – the distance from the centerline to the point (x, r), and R – the radius of the jet at a distance x from the fuel nozzle exit. If the small axial velocity on the boundary is denoted by v_b, we can write from eq. (10):

$$k_v = \ln\left(\frac{v_c}{v_b}\right) \tag{11}$$

Hence k_v depends on x. It should be noted that v_b is chosen arbitrarily by the user.

Applying the x component of the momentum equation to the control volume shown in fig. 2 yields:

$$\dot{m}_f v_f + \dot{m}_{a,inj} v_a = \rho_m (\alpha v_m^2)\pi R^2 \tag{12}$$

Here, ρ_m is the mean density of the jet at a distance x from the fuel nozzle exit. It is determined using the ideal gas law and mixture relations as:

$$\rho_m = \left(\frac{\dot{m}_f + \dot{m}_{a,inj} + \dot{m}_{a,ent}}{\dot{m}_f R_f + \dot{m}_{a,inj} R_a + \dot{m}_{a,ent} R_a}\right)\frac{p}{T} \tag{13}$$

In this equation, $\dot{m}_{a,ent}$ is the mass flow rate of air entrained into the jet from the ambient air, R_f – the gas constant of fuel, R_a – the gas constant of air, p – the operating pressure, and T – the temperature. In eq. (12), v_m is the mean axial velocity at a distance x from the fuel nozzle exit and α – the dimensionless momentum-flux correction factor. The factor α accounts for the variation of the axial velocity across the desired section of the jet. v_m is defined as $v_m \equiv (1/\pi R^2)\int_0^R v(2\pi r)\mathrm{d}r$.

Applying conservation of mass to the control volume shown in fig. 2, we obtain:

$$\dot{m}_f + \dot{m}_{a,inj} + \dot{m}_{a,ent} = \rho_m v_m \pi R^2 \tag{14}$$

From eqs. (10), (12), and (14), $\dot{m}_{a,ent}$ and R are obtained as follows:

$$\dot{m}_{a,ent} = -\dot{m}_f - \dot{m}_{a,inj} + \frac{(\dot{m}_f v_f + m_{a,inj} v_a)k_v}{\alpha v_c[1-\exp(-k_v)]} \tag{15}$$

$$R = \sqrt{\frac{(\dot{m}_f + \dot{m}_{a,inj} + \dot{m}_{a,ent})k_v}{\pi \rho_m v_c[1-\exp(-k_v)]}} \tag{16}$$

Since $\dot{m}_{a,ent}$ at $x = 0$ is zero, α must have the following value:

$$\alpha = \frac{(\dot{m}_{\mathrm{f}} v_{\mathrm{f}} + \dot{m}_{\mathrm{a,inj}} v_{\mathrm{a}}) \ln\left(\frac{v_{\mathrm{f}}}{v_{\mathrm{b}}}\right)}{(\dot{m}_{\mathrm{f}} + \dot{m}_{\mathrm{a,inj}})(v_{\mathrm{f}} - v_{\mathrm{b}})} \tag{17}$$

It is assumed that α is independent of x.

Thus, the mass flow rate of the entrained air and the boundary of the jet can be easily found from eqs. (15) and (16), respectively. In these equations, k_{v} and ρ_m are determined from eqs. (11) and (13).

Concentration field

In the present model, individual species concentrations are derived from the predicted mixture fraction distribution. The mixture fraction has been defined in the literature as:

$$f \equiv \frac{c_i - c_{i,\mathrm{a}}}{c_{i,\mathrm{f}} - c_{i,\mathrm{a}}}$$

where c_i is the atomic mass fraction for element i at any desired point, $c_{i,\mathrm{a}}$ – the atomic mass fraction for element i at the oxidizer (air) nozzle exit, and $c_{i,\mathrm{f}}$ – the atomic mass fraction for element i at the fuel nozzle exit. $f = 0$ and $f = 1$ imply the existence of pure oxidizer (air) and pure fuel, respectively.

Since the mechanisms of momentum and mass transfer are alike [13, 16, 17], radial distribution of the mixture fraction at any desired cross-section of the jet can be assumed to be similar to that of the axial velocity. That is:

$$\frac{f}{f_{\mathrm{c}}} = \exp\left[-k_{\mathrm{f}}\left(\frac{r}{R}\right)^2\right] \tag{18}$$

In the above relation, f is the mixture fraction at the point (x, r), and f_{c} – the mixture fraction on the symmetry axis at the point $(x, 0)$. We assume that $k_{\mathrm{f}} = \beta k_{\mathrm{v}}$ where β is a constant.

The mean mixture fraction at a distance x from the fuel nozzle exit can be calculated as:

$$f_{\mathrm{m}} = \frac{c_{i,\mathrm{m}} - c_{i,\mathrm{a}}}{c_{i,\mathrm{f}} - c_{i,\mathrm{a}}} \tag{19a}$$

The subscript m stands for mean. Prior to ignition, the atomic mass fractions in eq. (19a) can be replaced with the mass fractions of a reactant (*i. e.* fuel or oxidizer). The mean mass fraction of reactant i at a distance x from the fuel nozzle exit, $\hat{c}_{i,\mathrm{m}}$, can be found from the mass flow rates as $\hat{c}_{i,m} = \dot{m}_i/\dot{m}_{\mathrm{t}}$. Here $\dot{m}_i$ is the mass flow rate of reactant i and $\dot{m}_{\mathrm{t}}$ – the total mass flow rate at the desired cross-section of the jet. The mass fractions of reactant i at the fuel nozzle exit $\hat{c}_{i,\mathrm{f}}$ and at the oxidizer nozzle exit $\hat{c}_{i,\mathrm{a}}$ are known from the boundary conditions. Thus, the mean mixture fraction at a distance x from the fuel nozzle exit can be found as:

$$f_{\mathrm{m}} = \frac{\hat{c}_{i,\mathrm{m}} - \hat{c}_{i,\mathrm{a}}}{\hat{c}_{i,\mathrm{f}} - \hat{c}_{i,\mathrm{a}}} = \frac{\frac{\dot{m}_i}{\dot{m}_{\mathrm{t}}} - \hat{c}_{i,\mathrm{a}}}{\hat{c}_{i,\mathrm{f}} - \hat{c}_{i,\mathrm{a}}} \tag{19b}$$

On the other hand, the mean mixture fraction is defined as:

$$f_{\mathrm{m}} \equiv \frac{1}{\pi R^2} \int_0^R f\,(2\pi r)\mathrm{d}r \tag{20}$$

Mixture fraction on the centerline of the jet can be obtained using eqs. (18) to (20):

$$f_c = \frac{\beta k_v f_m}{[1-\exp(-\beta k_v)]} \tag{21}$$

At $x = 0$, f_c, k_v, and f_m are known. Thus, β can be readily found. Once β is found, the mixture fraction at any desired point on the symmetry axis of the jet can be determined from eq. (21).

The small value of the mixture fraction on the boundary of the jet is obtained from eqs. (10) and (18) at $x = 0$ as $f_b = (v_b/v_f)^\beta$.

As will be shown in the next section, values of f_c predicted by eq. (21) can be modified to agree with the CFD solution and experimental data more reasonably, using the following correction function:

$$\mathrm{f}_{\mathrm{corr}} = \begin{cases} \mathrm{f}_{\mathrm{corr},1}, & x < x_1 \\ c_0 + c_1 x + c_2 x^2, & x_1 \le x \le x_2 \\ \mathrm{f}_{\mathrm{corr},2}, & x > x_2 \end{cases} \tag{22}$$

Different parameters in the recent relation are:

$$\mathrm{f}_{\mathrm{corr},1} = 1, \quad x_1 = L_{\mathrm{core}}, \quad \mathrm{f}_{\mathrm{corr},2} = \frac{1}{k_0 + k_1 (MR)}, \quad k_0 = 1.5075, \quad k_1 = 1.2900, \quad x_2 = 30 d_{\mathrm{e}}$$

$$\mathrm{c}_2 = \frac{\mathrm{f}_{\mathrm{corr},1} - \mathrm{f}_{\mathrm{corr},2}}{(x_1 - x_2)^2}, \quad c_1 = -2 c_2 x_2, \quad c_0 = \mathrm{f}_{\mathrm{corr},1} - c_1 x_1 - c_2 x_1^2$$

It is observed that the minimum value of the correction function $\mathrm{f}_{\mathrm{corr},2}$ depends mainly on the momentum ratio. Thus, it is found in several cases with different momentum ratios from the CFD solution. Then k_0 and k_1 are determined using the least squares method. This is demonstrated in fig. 3. L_{core} is the length of the potential core, and d_{e} is the equivalent nozzle diameter [16]:

$$d_{\mathrm{e}} = \frac{2(\dot{m}_{\mathrm{f}} + \dot{m}_{\mathrm{a,inj}})}{\sqrt{\pi \rho_{\mathrm{e}} (\dot{m}_{\mathrm{f}} v_{\mathrm{f}} + \dot{m}_{\mathrm{a,inj}} v_{\mathrm{a}})}}$$

where ρ_{c} is the equivalent fluid density, that is:

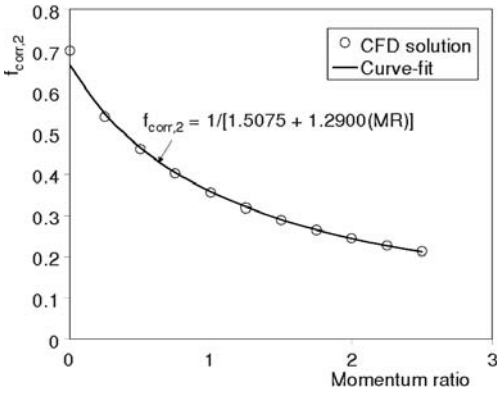

Figure 3. Curve-fit expression for the minimum value of the correction function $\mathrm{f}_{\mathrm{corr},2}$

$$\rho_{\mathrm{e}} = \frac{\dot{m}_{\mathrm{f}} \rho_{\mathrm{f}} + \dot{m}_{\mathrm{a,inj}} \rho_{\mathrm{a}}}{\dot{m}_{\mathrm{f}} + \dot{m}_{\mathrm{a,inj}}}$$

Modified values of the mixture fraction on the centerline of the jet $\mathrm{f}_{\mathrm{c,mod}}$ are calculated multiplying the values predicted by eq. (21) by the correction function:

$$f_{\mathrm{c,mod}} = \mathrm{f}_{\mathrm{corr}} f_{\mathrm{c}} \tag{23}$$

Radial distribution of the mixture fraction at any desired cross-section of the jet is obtained from eq. (18) the same as before, except that β is assumed to be equal to 1 and, in turn, $k_{\mathrm{f}} = k_{\mathrm{v}}$.

Obviously, this time the modified values of the mixture fraction on the symmetry axis are used. Therefore, eqs. (18) and (21) to (23) provide all the information on species concentration distribution we need.

CFD computations

The CFD computations are based on the numerical solution of the continuity, momentum, and turbulence model equations as well as the chemical species transport equations. Turbulent viscosity is determined using the two-equation Realizable k-ε model because this model addresses the deficiencies of the traditional k-ε models. For example, the Realizable k-ε model satisfies certain mathematical constraints on the normal stresses, consistent with the physics of turbulent flows. The modeled equation for the dissipation rate ε and the eddy-viscosity formula are also improved in the Realizable k-ε model. Thus the performance of the Realizable k-ε model is substantially better than that of the traditional k-ε models, especially for flows involving rotation, re-circulation, strong streamline curvature, and planar and round jets [18-21]. More details about the equations are given in [18, 19].

The calculations are carried out using the flow solver Fluent 6.2. All the governing equations are discretized using the second order upwind scheme. The discretized equations are solved using the Simple algorithm. The implicit and segregated solver is applied for the solution of the system of governing equations. The software Gambit 2.2 is employed to generate the geometry and mesh for the computational domain. The computational domain is a 350 mm × 1500 mm rectangular.

Because of the symmetry of the coaxial jets about their axis, they can be treated as 2-D for the purpose of analysis. Hence the computations are performed on 2-D meshes. Three progressively finer meshes are used to secure grid independence. Results are virtually identical for the three meshes and the minor grid dependence of the results are safely neglected. The chosen mesh consists of 6550 quadrilateral cells. To capture the details of the flow accurately, the size of the cells are significantly reduced near the air and fuel nozzles and also the symmetry axis where large gradients are expected. This 2-D mesh is shown in fig. 4.

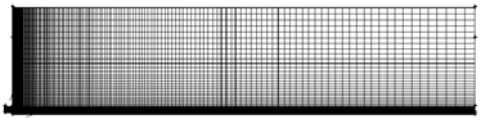

Figure 4. The 2-D mesh used in the CFD computations consisting of 6550 quadrilateral cells

Velocity inlet boundary condition is used at the exit of the fuel and air nozzles and pressure inlet/outlet boundary condition is used at the limits of the computational domain. At the symmetry axis, axis boundary condition is used. Wall boundary condition with constant temperature of 300 K and no-slip condition is used at the nozzle walls. Convergence criterion for all the governing equations is the residual value. Solution is considered to be converged when the residual values become less than 10^{-4}. It takes about 20 minutes for each solution to converge. Turbulence intensity is assumed to be 10% at the exit of the fuel and air nozzles. Turbulence kinetic energy k and its dissipation rate ε are set to zero at the pressure boundaries.

Results and discussion

Results of the present model are validated by the measurements of Warda *et al.* [10] for the velocity distribution and by the experimental data of Birch *et al.* [17] for the concentration field. Warda *et al.* [10] have reported measurements of the flow field of coaxial air jets with the inner-to-outer stream velocity [ms^{-1}] ratio of 10/5 and the inner-to-outer nozzle diameter [mm] ratio of 7/15. Radial distribution of the axial velocity has been reported at $x/d_1 = 9.25$. Birch *et*

al. [17] have measured the mass fraction of methane in a round methane jet issuing from a tube of diameter 12.65 mm with a velocity of 19.40 m/s.

Results are also compared with those obtained using the semi-empirical relations of Beer and Chigier [16] in the fully developed region and with the CFD solution wherever possible. Results of the present model for coaxial methane-air jets with the fuel-to-air discharge velocity [ms^{-1}] ratio of 20/2.15 and the fuel-to-air nozzle diameter [mm] ratio of 10/50 are presented as samples.

Figure 5 shows the velocity decay along the centerline of the coaxial air jets. It can be seen that the results of the present model are in very good agreement with the measurements of Warda *et al.* [10], especially after $x/d_1 \approx 8$. Radial distribution of the axial velocity at $x/d_1 = 9.25$ is shown in fig. 6. Results of the present model are almost identical with the experimental data of Warda *et al*. [10] up to $r/d_1 \approx 1$ and are slightly lower in the outer region of the jet.

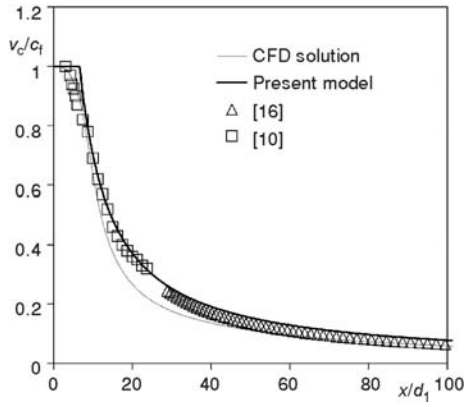

Figure 5. Velocity decay along the centerline of the coaxial air jets

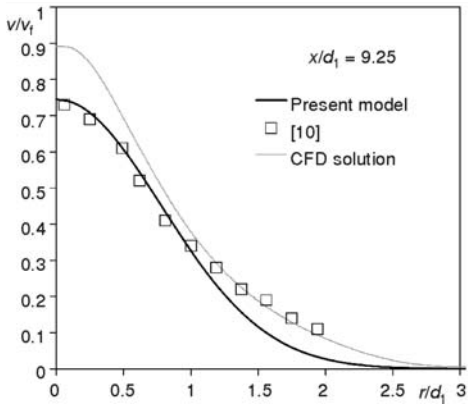

Figure 6. Radial distribution of the axial velocity at $x/d_1 = 9.25$ of the coaxial air jets

Figure 7 represents the mixture fraction on the centerline of the round methane jet. As shown in this figure, results of the present model are considerably modified using eq. (22), after $x/d_1 \approx 30$. Very good agreement is observed in this region. Before $x/d_1 \approx 30$, the values predicted by the present model (with or without modification) are a bit lower than those measured by Birch *et al*. [17].

In fig. 8, variation of the velocity along the symmetry axis of the coaxial methane-air jets is shown. All the three curves are virtually identical. Only a slight difference in the length of the potential core can be observed very close to the nozzle exit.

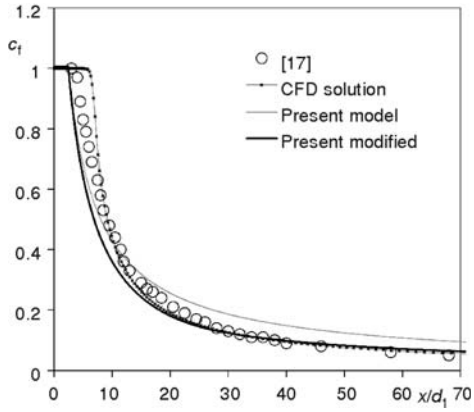

Figure 7. Mixture fraction on the centerline of the round methane jet

Figure 9 demonstrates the radial distribution of the axial velocity in the fully developed region of the coaxial methane-air jets at $x/d_1 = 80$. As can be seen, the axial velocities predicted by the present model are somewhat lower than those predicted by Beer and Chigier [16], up to

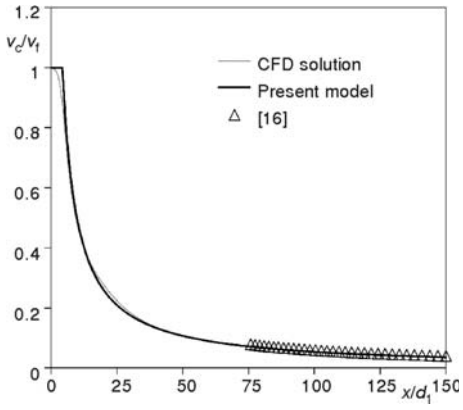

Figure 8. Variation of the velocity along the symmetry axis of the coaxial methane-air jets

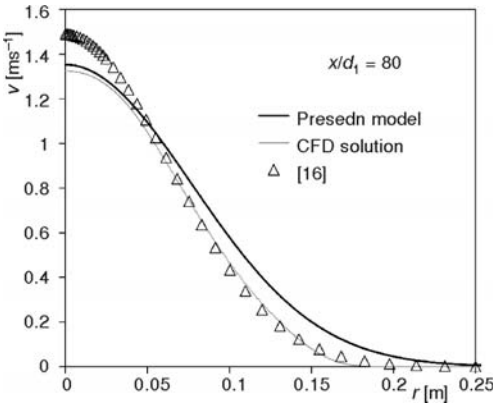

Figure 9. Radial distribution of the axial velocity at $x/d_1 = 80$ of the coaxial methane-air jets

about $r = 0.05$. From that point onwards, the reverse is true. In the present model, the axial velocity approaches zero more slowly than in the other works.

Figure 10 shows the mixture fraction on the centerline of the coaxial methane-air jets. Although the present model over-predicts the mixture fraction on the centerline, it provides good results after modification, especially after about $x/d_1 \approx 50$. Results of the CFD solution are somewhat lower than those of the present model with or without modification, in the near-field region of the jet (*i. e.* $x/d_1 < 50$).

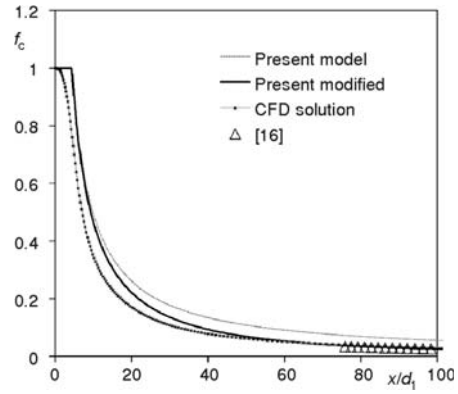

Figure 10. Mixture fraction on the centerline of the coaxial methane-air jets

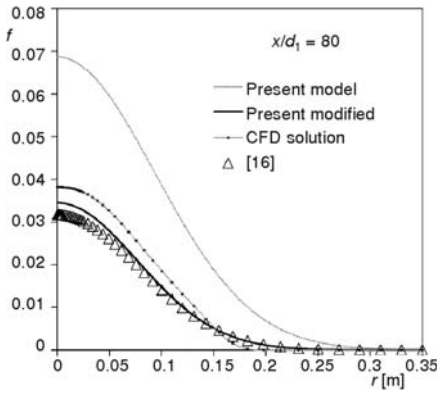

Figure 11. Radial distribution of the mixture fraction at $x/d_1 = 80$ of the coaxial methane-air jets

Radial distribution of the mixture fraction in the fully developed region of the coaxial methane-air jets at $x/d_1 = 80$ is shown in fig. 11. The values predicted by the present model (without modification) are significantly higher than those predicted by Beer and Chigier [16] and the CFD solution. This is traced back to an over-prediction of the mixture fraction on the jet centerline. However, the modified model provides much better results which are in very good agreement with those of Beer and Chigier [16]. Predicted values of the mixture fraction near the symmetry axis are slightly higher in the modified model than those of Beer and Chigier [16].

According to the results, the presented model can reasonably predict the behavior of turbulent coaxial gaseous jets and provide sufficiently accurate estimates of the flow and concentration fields, in a very short time (about 4 seconds).

Conclusions

In this work, a semi-analytical model for the prediction of the behavior of turbulent coaxial gaseous jets is presented. Simple relations which can be easily applied to all the regions of the jets are proposed to predict the flow and concentration fields. The model is also capable of predicting the behavior of single round jets. CFD simulations are carried out to yield further insights into the problem using the flow solver Fluent 6.2. The continuity and momentum equations as well as the ideal gas equation of state are employed to derive the desired expressions. Curve-fits to the CFD solutions are used to determine the experimental constants. A computer program is developed in Matlab 7.1 to implement the presented model. The time required by the presented model is about $1/300^{th}$ of that required by the CFD solution. Results are compared with existing data and reasonable agreement is observed.

References

[1] Forstall, W., Shapiro, A. H., Momentum and Mass Transfer in Coaxial Gas Jets, *Journal of Applied Mechanics, 18* (1950), 2, pp. 399-408
[2] Morton, B. R., Coaxial Turbulent Jets, *International Journal of Heat and Mass Transfer, 5* (1962), 10, pp. 955-965
[3] Chigier, N. A., Beer, J. M., The Flow Region Near the Nozzle in Double Concentric Jets, *Journal of Basic Engineering, 86* Series D (1964), 4, pp. 797-804
[4] Williams, T. J., *et al*., Noise and Flow Characteristics of Coaxial Jets, *Journal of Mechanical Engineering Science, 11* (1969), 2, pp. 133-142
[5] Champagne, F. H., Wygnanski, I. J., An Experimental Investigation of Coaxial Turbulent Jets, *International Journal of Heat and Mass Transfer, 14* (1971), 9, pp. 1445-1464
[6] Ribeiro, M. M., Whitelaw, J. H., Turbulent Mixing of Coaxial Jets with Particular Reference to the Near-Exit Region, *Journal of Fluids Engineering-Transactions of the ASME, 98* (1976), 2, pp. 284-291
[7] Ko, N. W. M., Kwan, A. S. H., The Initial Region of Subsonic Coaxial Jets, *Journal of Fluid Mechanics, 73* (1976), 2, pp. 305-332
[8] Dahm, W. J. A., *et al*., Vortex Structure and Dynamics in the Near Field of a Coaxial Jet, *Journal of Fluid Mechanics, 241* (1992), August, pp. 371-402
[9] Buresti, G., *et al*., Experimental Investigation on the Turbulent Near-field of Coaxial Jets, *Experimental Thermal and Fluid Science, 17* (1998), 1-2, pp. 18-26
[10] Warda, H. A., *et al*., Influence of the Magnitude of the Two Initial Velocities on the Flow Field of a Coaxial Turbulent Jet, *Flow Measurement and Instrumentation, 12* (2001), 1, pp. 29-35
[11] Schumaker, S. A., An Experimental Investigation of Reacting and Nonreacting Coaxial Jet Mixing in a Laboratory Rocket Engine, Ph. D. thesis, University of Michigan, Ann Arbor, Mich., USA, 2009
[12] Enjalbert, N., *et al.*, An Entrainment Model for the Turbulent Jet in a Coflow, *Comptes Rendus Mecanique, 337* (2009), 9-10, pp. 639-644
[13] Antoine, Y., *et al.*, Turbulent Transport of a Passive Scalar in a Round Jet Discharging into a Co-flowing Stream, *European Journal of Mechanics B-Fluids, 20* (2001), 2, pp. 275-301
[14] Belosevic, S., *et al.*, Three-dimensional Modeling of Utility Boiler Pulverized Coal Tangentially Fired Furnace, *International Journal of Heat and Mass Transfer, 49* (2006), 19-20, pp. 3371-3378
[15] Kandakure, M. T., *et al*., Characteristics of Turbulent Confined Jets, *Chemical Engineering and Processing, 47* (2008), 8, pp. 1234-1245
[16] Beer, J. M., Chigier, N. A., *Combustion Aerodynamics*, Applied Science Publishers, London, 1972
[17] Birch, A. D., *et al*., The Turbulent Concentration Field of a Methane Jet, *Journal of Fluid Mechanics, 88* (1978), 3, pp. 431-449
[18] Shih, T. H., *et al*., A New k-ε Eddy-Viscosity Model for High Reynolds Number Turbulent Flows: Model Development and Validation, *Computers & Fluids, 24* (1995), 3, pp. 227-238
[19] ***, Fluent 6.2 User's Guide, Fluent Inc., Lebanon, NH 03766, USA, 2005

[20] Khalilarya, Sh., *et al*., Evaluation of Two-Equation Turbulence Models for the Simulation of Gaseous Round Jets (in Farsi), *Proceedings*, Mechanical Engineering Conference, Mashhad, Iran, 2009, p. 210
[21] Khalilarya, Sh., Lotfiani, A., Determination of Flow Pattern and its Effect on NO_x Emission in a Tangentially Fired Single Chamber Square Furnace, *Thermal Science, 14* (2010), 2, pp. 493-503

Paper submitted: July 1, 2011
Paper revised: July 4, 2012
Paper accepted: July 11, 2012